

AperTO - Archivio Istituzionale Open Access dell'Università di Torino

Multi-scale remote sensing to support insurance policies in agriculture: from mid-term to instantaneous deductions

This is the author's manuscript

Original Citation:

Availability:

This version is available <http://hdl.handle.net/2318/1754975> since 2020-09-04T16:32:18Z

Published version:

DOI:10.1080/15481603.2020.1798600

Terms of use:

Open Access

Anyone can freely access the full text of works made available as "Open Access". Works made available under a Creative Commons license can be used according to the terms and conditions of said license. Use of all other works requires consent of the right holder (author or publisher) if not exempted from copyright protection by the applicable law.

(Article begins on next page)

**Multi-Scale Remote Sensing to Support Insurance Policies in Agriculture:
from Mid-Term to Instantaneous Deductions**

Sarvia, F.^{a*}, De Petris S.^a, Borgogno-Mondino, E.^a

^aDepartment of Agricultural, Forest and Food Sciences, University of Turin, Italy.

**filippo.sarvia@unito.it*

1 **Multi-Scale Remote Sensing to Support Insurance Policies in Agriculture:** 2 **from Mid-Term to Instantaneous Deductions**

3 4 **Abstract**

5 Climate change is today one of the biggest issues for farmers. The increasing number of natural
6 disasters and change of seasonal trends is making insurance companies more interested in new
7 technologies that can somehow support them in quantifying and mapping risks. Remotely sensed data,
8 with special focus on free ones, can certainly provide the most of information they need, making
9 possible to better calibrate insurance fees in space and time. In this work, a prototype of service based
10 on free remotely sensed data is proposed with the aim of supporting insurance companies' strategies.
11 The service is thought to calibrate annual insurance rates, longing for their reduction at such level that
12 new customers could be attracted. The study moves from the entire Piemonte region (NW Italy), to
13 specifically focus onto the Cuneo province (Southern Piemonte), that is mainly devoted to agriculture.
14 MODIS MOD13Q1-v6 and Sentinel-2 L2A image time series were jointly used. NDVI maps from
15 MODIS data were useful to describe the midterm phenological trends of main crops at regional level
16 in the period 2000-2018; differently, Sentinel-2 data permitted to map local crop differences at field
17 level in 2016 and 2017 years. With reference to MODIS data, the average phenological behaviour of
18 main crop classes in the area, obtained from the CORINE Land Cover map Level 3, was considered
19 using a time series decomposition approach. Trend analyses showed that the most of crop classes
20 alternated three phases (about 7 years) suggesting that, presently, this is probably the time horizon to
21 be considered to tune mid-term algorithms for risk estimates in the agricultural context. Crop classes
22 trends were consequently split into 3 phases and each of them modelled by a 1st order polynomial
23 function used to update correspondent insurance risk rate. Sentinel-2 data were used to map
24 phenological anomalies at field level for the 2016 and 2017 growing seasons; shifts from class average
25 behaviour were considered to locally and temporarily tune insurance premium around its average trend
26 as described at the previous step. Synthesizing, one can say that this approach, integrating MODIS and
27 Sentinel-2 data, makes possible to locally and temporarily calibrate premiums of indexed insurance
28 policies by describing the average trends of crop performance (NDVI) at regional level by MODIS
29 data and refining it at field and specific crop level by Sentinel-2 data.

30 **Introduction**

31 Climate change is today one of the biggest issues for farmers. Every year natural
32 disasters hit the agricultural business with cost of billions of dollars. Drought is the most
33 significant threat, followed by floods, forest fires, storms, pests, pathogens, and others. The

34 United Nations Food and Agriculture Organization (FAO) (Conforti, Ahmed, and Markova
35 2018) claims that between 2005 and 2015, natural disasters brought \$ 96 billion of costs in
36 damaged or lost crops to the agricultural sectors of developing countries. Drought, which
37 affected farmers in all over the world, was one of the main culprits. 29 billion dollars are the
38 economic losses documented by FAO caused by drought (Baas, Trujillo, and Lombardi 2015;
39 FAO 2007).

40 Drought is also one of the most complex climatic phenomena among those affecting
41 the society and the environment (Wilhite 1993; Wilhite 2012). In Europe it is a recurring
42 event that does not hits the Mediterranean region only, but also occur in areas with high
43 rainfall and in any season (Estrela, Peñarrocha, and Millán 2000). The drought has been the
44 most serious climate risk of the twentieth century, responsible for the loss of billions of US
45 dollars (White 1994). It represents an extreme climate event, which varies in severity and
46 duration on all continents, causing critical damage to the natural environment and human lives
47 (Min et al. 2003; Modarres 2007). The future ecosystem changes and impacts on plants have
48 been extensively analyzed (Easterling et al. 2000; Meir and Grace 2006). However,
49 documented evidence of the effects of climate change on crop production has only recently
50 been provided (Lobell and Asner 2003; Chmielewski, Müller, and Bruns 2004, Tao et al.
51 2006; Zhang et al. 2019; Grillakis 2019).

52 During the last century large areas of Europe have been affected by this phenomenon.
53 The severe and prolonged periods of drought have highlighted the vulnerability of our
54 continent to this natural risk, evidencing to the public, governments and operating agencies
55 various socio-economic problems that accompany water scarcity and the need for measures to
56 mitigate their effects.

57 In relation to vegetation activity and crop productivity, Potop (2011) compared several
58 indices to evaluate its impact on maize crops in Moldova. Mavromatis (2007) and Quiring

59 and Papakryiakou (2003) similarly tried to quantify respectively its effects on wheat
60 production in Greece and Canadian prairies. Results from different studies differ each other,
61 depending on the drought index used to detect impacts. Consequently, a high uncertainty still
62 persists among scientists, managers and end users while selecting the proper index for
63 analysis. The amount of proposed indices and indicators for agricultural drought, or other
64 natural disasters, detection makes the decision-making process complicated. This complexity
65 may cause delayed, uncompleted or unwanted answers. These situations determine negative
66 economic consequences and generate loss of confidence in authorities that are responsible for
67 mitigation actions.

68 Real time drought monitoring based on few field data is a challenge for ecosystem
69 management and conservation. The most of methods require extensive data collection and in-
70 situ calibration and accuracy may be difficult to be quantified. The imbalance between
71 potential evaporation and the amount of precipitation during the growing season usually
72 causes drought conditions that can pose a threat to both the environment and human activities.
73 Thus, it is necessary to collect frequent information about drought severity and its spatial and
74 temporal distribution for mitigating its effects. Many studies have already explained the
75 important role of remote sensing in agriculture (Colwell et al. 1970; Bastiaanssen, Molden
76 and Makin 2000; Steven and Clark 2013; Atzberger 2013; Sahoo, Ray and Manjunath 2015;
77 Shanmugapriya et al. 2019; Weiss, Jacob and Duveiller 2020), others begun the
78 experimentation of monitoring catastrophic events using satellite data (Silleos, Perakis and
79 Petsanis 2002; Sandholt et al. 2003; Sanyal and Lu 2004; Rhee, Im and Carbone 2010; Rojas,
80 Vrieling and Rembold 2011) and, more specifically, spectral indexes such as the EVI
81 (Enhanced Vegetation Index), SAVI (Soil-Adjusted Vegetation Index), NDVI (Normalized
82 Difference Vegetation Index) and others more (Zhang et al. 2005; Beerli and Peled 2006;
83 Chen et al. 2006; Son et al. 2014; Sánchez et al. 2018; Lu, Carbone, and Gao 2019; Nanzad et

84 al. 2019). For this work, NDVI was selected as reference spectral index to base crop
85 performance monitoring on. In spite of some well-known limits (e.g. saturation in highly
86 vegetated areas), NDVI is certainly the most famous and used vegetation index for biomass
87 and crop productivity estimation; moreover, many EO (Earth Observation) data suppliers
88 make available ready-to-use maps of NDVI as free and immediately downloadable products
89 (e.g. MODIS derived MOD13Q1 product from USGS). These can be easily structured within
90 long time series stacks that ensure homogeneity of pre-processing, i.e. a higher comparability
91 of values and reliability of deductions. Standardization, convenience and ease of use of data
92 are extremely important factors for those users, like insurance companies, that are not familiar
93 with this type of technology.

94 Free satellite data from National Aeronautics and Space Administration (NASA)
95 TERRA and European Space Agency (ESA) Sentinel 2 (S2) missions were used to describe
96 agriculture crops growing steps and to protect and facilitate all the parts involved. Optical
97 data proved to be effective in describing vegetation development. In particular, free optical
98 data like Moderate Resolution Imaging Spectroradiometer (MODIS) and S2 ones is extremely
99 important and strategic in a low-income economical sector like the agricultural one since
100 further additive costs deriving from monitoring services could compromise competitiveness
101 of the entire sector (Borgogno and Gajetti 2017). Information obtained from free monitoring
102 services may represent a helpful tool for farmers, making them able to improve ordinary
103 management strategies and move to a higher environmental sustainability of agriculture. As
104 Islam et al., (2017) affirms that the implementation of knowledge about the development and
105 phenology of crops into the classification process introduces further possibilities for
106 improving crop monitoring.

107 All this said, is worth to remind that Italy was one of the first countries to tackle the
108 issue of risk management in agriculture, introducing, with the National Solidarity Fund

109 (FSN), the principle of solidarity for those companies suffering from damage caused by
110 natural disasters. FSN involves compensatory interventions when a damage occurs by adverse
111 events. Ground controls and delimitation of affected areas are mandatory. Envisaged
112 measures mainly consist of contribution to agricultural companies that suffered from a yield
113 loss higher than the 35% out of the total (Borriello 2003). Active defense has the purpose of
114 safeguarding crop production, preventing or neutralizing the negative effects of calamitous
115 events through technological devices, such as anti-freeze fans and exploding rockets, to
116 dissolve hailstorms. Differently, facilitated insurance policies focus on risk prevention. The
117 State intervenes with a contribution partially covering insurance fees paid by the farmer. The
118 Minister for Agricultural Policies with the 28405/17 decree extend insurance coverage even
119 further with subsidized policies (indexed insurance policies) against damage from adverse
120 weather conditions to crops, but also for damage to structures or livestock. The decree
121 indicates in Annex 1 the crops, the company structures and the types of insurable cattle. Crops
122 such as corn, wheat and lawn are included in this list. The new policies offer insurance
123 packages that are not available on the market. They are intended to encourage Italian farmers
124 to insure themselves to overcome climate risks.

125 In France, the policy against new climate risks is the one that has grown most in recent
126 years, reaching a coverage of 30% of the surface area (Chenet 2019). Globally, the
127 agricultural insurance market is concentrated in high-income agricultural countries, with the
128 US alone accounting for 38% of premiums. In Italy, against the atmospheric phenomena that
129 threaten crops, few choose to protect the territory. Climate change is slowly persuading Italian
130 farmers to increase the use of policies against atmospheric risks, albeit with large differences
131 in areas and crops. The first case came two years ago, in the horrible 2017, devastated by frost
132 and drought, which has increased the compensation paid by farms. The presence of extreme
133 weather events has become the norm and, according to Coldiretti (the largest association

134 representing and assisting Italian agriculture), has weighed Italian agriculture more than 14
135 billion in a decade between production losses and damage to structures and infrastructure in
136 the countryside (Hay 2019; Severini, Biagini, and Finger 2019). In Italy, only 78,000
137 companies are insured, 9% of the total, representing 8.3% of the national agricultural area and
138 18.7% of production. There is a deep gap between the areas of Central-Northern Italy and
139 Southern Italy, which still represents, according to the latest Ismea report, only 12% of farms
140 insured at national level (De Ruvo et al. 2019). The farmer is still interested in the small
141 damage, when more and more often an extended catastrophe risks destroy entire farms.

142 This paper focuses on the so called *indexed* (experimental) insurance policies, trying
143 to calibrate an insurance risk model relaying on time series of spectral indexes map (e.g.
144 NDVI) from remotely sensed data.

145 **Material and methods**

146 *Study area*

147 The study area is located in Piemonte, North-West Italy (fig. 1). It sizes about 25388
148 km² and well represents a typical agricultural context of northern Italy. Climate is temperate
149 with a continental character, where North-Western Alps cause a gradual reduction of
150 temperature while altitude increases. Yearly average rainfall gauge is 930 mm and yearly
151 average temperature is 11.9 °C. Thermal inversion phenomena caused by cold air can often
152 affect the area.

153 [FIGURE 1]

154 The focus area is located within the Cuneo province including the following
155 municipalities: Cuneo, Fossano, Castelletto Stura, Margarita, Trinità, Sant'Albano Stura,
156 Centallo, Montanera, Rocca de Baldi and Morozzo (fig. 1). The soil is locally characterized
157 by a high permeability and a good availability of oxygen due to the texture, rich in sands
158 (averagely > 50%) and to the skeleton, poor in clay. Soil depth for root development is low

159 due to the high presence of gravel. This work was focused on the following crop classes:
160 wheat, corn, meadow, ryegrass, that represent about 48% of the total area (table 1).

161 [TABLE 1]

162 *Available data*

163 The following data were used to test the proposed procedure: a) satellite multispectral
164 images from NASA TERRA MODIS and Copernicus S2 Multi Spectral Instrument (MSI)
165 sensors; b) 2012 CORINE Land Cover Map; c) a vector cadaster map; d) a vector
166 administrative boundaries map; e) farmers' applications for EU incentives within CAP.

167 *Satellite data*

168 In this work satellite data were intended to respond to two main tasks in the context of
169 insurance for crops. The first one was to look at mid-term trends of crop performances at
170 regional level, requiring elongated image time series able to describe the average behavior of
171 macro-classes of crop types. For this purpose, low resolution satellite data from MODIS
172 sensor, operating on board of the TERRA satellite mission since 2000, were considered.

173 To opportunely tune crop performances around their average trend at year level and
174 mapping intra-classes differences at field level, a higher geometric resolution was retained
175 more appropriate to fit the local average size of fields. For this task, data from the Copernicus
176 Sentinel 2 mission were adopted.

177 With reference to MODIS data, the MOD13Q1-v6 product from Land Processes
178 Distributed Active Archive Center (LPDAAC) collection of NASA (Solano et al., 2010) was
179 used to generate a 432 images time series (hereinafter called TS) of NDVI (Rouse et al. 1974)
180 covering the period 2000 - 2018. Data were obtained from the AppEEARS system (Didan
181 2015), georeferenced in the WGS84 geographic reference frame and supplied in Tagged
182 Image File (TIF) format. The MOD13Q1-v6 data are 16 days timely-spaced and have a
183 spatial resolution of 250 m. The MOD13Q1-v6 product is composed of all the best available

184 local observations (at pixel level) out of those available in the considered 16 days period.
185 Selection criteria take into account cloud cover (lower), viewing angles (lower) and NDVI
186 local value (maximum in the reference period). A pixel reliability layer (PR) is also available
187 from the MOD13Q1-v6 mapping the following codes: -1 = No Data, 0 = Good Data, 1 =
188 Marginal data, 2 = Snow/Ice, 3 = Cloudy.

189 With reference to the Sentinel 2 mission, 31 Sentinel 2 Level-2A data were obtained from the
190 Theia system (theia.cnes.fr). They were obtained as 100 x 100 km² tiles orthoprojected into
191 the WGS84 UTM 32N reference frame (Sentinel-2 User Handbook; 2015). Level-2A
192 products were supplied already calibrated in "at-the-Bottom of the Atmosphere" reflectance
193 (BOA), guaranteeing immediate usability for land applications. Table 2 shows the main
194 technical specifications of both MODIS and S2 MSI (Multi Spectral Instrument) sensors.

195 [TABLE 2]

196 *Auxiliary data*

197 The 2012 CORINE Land Cover dataset level 3 (hereinafter CLC2012) was used to
198 map cultivated areas over Piemonte. CLC2012 was obtained, for free, from the Land
199 Monitoring Service Copernicus. Technical features of CLC2012 are reported in table 3.
200 According to the CLC2012 nomenclature, the level 3 is the most detailed level in the
201 hierarchical classification system adopted by CORINE Land Cover project. This level maps
202 homogeneous landscape patterns having more than 75% of the characteristics of a given class
203 according to the nomenclature rules (Büttner 2014). With reference to agricultural classes,
204 table 4 reports the list of the agricultural classes as coded in CLC2012 Level 3 that were
205 considered for this work.

206 [TABLE 3]

207 [TABLE 4]

208 Farmers' declaration for European incentives of the years 2016 - 2017, was used to
209 find and locate the cultivated crops in the study area. Farmers apply every year to receive EU
210 contributions supporting their activity. A database containing farmers' applications is
211 currently made available by the Piemonte Region institutional website (Sistema Piemonte)
212 and can be downloaded at municipal level (MO Excel format).

213 A vector format cadastral map (2018 updated, nominal scale 1:2000), mapping parcels
214 in the study area, was used to geolocate farmers' applications. This made possible to generate
215 an official administratively-based map of existing crops in the area. Cadastral map was
216 obtained by the Piemonte Region Geoportal already georeferenced in the WGS84 / UTM
217 zone 32N reference frame.

218 A vector map of administrative boundaries (2019 updated, scale 1:100000) was also
219 obtained from the Piemonte Region Geoportal.

220 *NDVI Time Series Generation*

221 NDVI is well known to be a spectral index useful for retrieving vegetation canopy
222 biophysical properties (Leprieur, Verstraetel and Pinty 1994; Jonsson and Eklundh 2002).
223 According to some recent studies it could also be used for supporting remotely sensed-based
224 crop insurance models (Jensen et al. 2019; Sarvia, De Petris, and Borgogno 2019) being a
225 good predictor of crop yield (Haghverdi, Washington-Allen, and Leib 2018; Zambrano et al.
226 2018). Although many other indices from remotely sensed data are suggested in literature for
227 vegetation monitoring, as we have specified in the introduction, we decided to focus on NDVI
228 according the following criteria: a) the study area (Piemonte Region) highly suffers from haze
229 (both natural and anthropic) for many months along the growing season. Consequently,
230 spectral indices able to minimize these effects are mostly desirable. It can be mathematically
231 proved that indices defined in term of ratios (or ratios of differences), with no additive terms
232 (often empirical), are the most promising ones being able to minimize this effect, whose

233 consequence, in data interpretation, is especially high when working with index time series.
234 Consequently, attention was addressed to these types of vegetation indices (slope based like
235 NDVI, NDRE, NDWI, etc.), driving to exclude other ones like EVI, PVI, SAVI, MSAVI,
236 EVI. With these premises and with reference to the TERRA MODIS MOD13Q1 product used
237 in this work (only containing NDVI and EVI grids) to describe vegetation trends in the mid-
238 term period, NDVI was the best candidate. Moreover, NDVI permits an easier integration
239 with data from UAVs (Unmanned Aerial Vehicles) and UGV (Unmanned Ground Vehicles)
240 that, ordinarily, are equipped with low cost multispectral sensors that, minimally, can record
241 red and NIR bands needed to derive the correspondent NDVI map. This issue, presently,
242 cannot be neglected given the ongoing improvement and spreading of remote sensing based
243 precision farming techniques (Borgogno and Gajetti 2017).

244 With reference to the MOD13Q1-v6 product, a regularly timely spaced MODIS NDVI
245 TS (about 23 images/year, one image every 16 days) can be easily obtained. Consequently, a
246 NDVI TS of 432 maps (hereinafter called MOD_TS) was generated exploring the period
247 2000–2018.

248 As far as S2 data are concerned two annual NDVI TS were generated for the 2016 and
249 2017 agronomic seasons for a total of 31 “good” images (a filter was applied to exclude
250 images showing in the study area a percentage of cloud cover > 20%). S2 band 8 (wide band
251 NIR) and band 4 (Red band) were used for NDVI computation. S2 native NDVI TS was pre-
252 processed removing “bad” observations from the local NDVI temporal profile of each pixel
253 and densifying the TS 5 days regularly spaced one. Both the operations were achieved
254 contemporarily by a self-developed IDL (Interactive Data Language) routine. Filtering was
255 operated by exclusion with reference to the quality layer supplied with the BOA S2 product.
256 S2 TS densification/regularization was obtained by spline interpolation with tensor (value =
257 10) applied at pixel level. Finally, the new pre-processed S2 TS was made of 146 NDVI maps

258 5 days regularly spaced (hereinafter called S2_TS). S2_TS was split in two stacks, singularly
259 representing the two considered years (2016 and 2017). Splitting was operated according to
260 the so called “agronomic year”, i.e. the period ranging from November to November of two
261 consequent years (starting on 11th November).

262 *Analyzing Crops Performance*

263 Assuming insurance risk associated with the expected performance of crops, a simplified
264 procedure for updating risk estimates based on NDVI TS from both low (MODIS) and high
265 (S2) resolution satellite imagery was developed, with reference to the two above mentioned
266 levels of investigation: trend and tuning.

267 Trend analysis was based on MOD_TS and it was operated at crop (macro-) class
268 level, improving the method previously proposed by Borgogno, Sarvia and Gomasca
269 (2019). Consequently, according to the considered CLC2012 crop classes (table 4) the
270 average NDVI temporal profile was computed for each class by ordinary zonal statistics
271 available in QGIS 3.10. The obtained sixteen days-spaced mean class temporal profiles were
272 then aggregated at year level by computing the yearly 95th percentile. New profiles
273 (hereinafter called PR95Y) containing one value per year (2000-2018) were obtained and
274 analyzed by time decomposition with the aim of extracting the dominant trends (low
275 frequency variations) underlying the entire profile. The adoption of 95th percentile as
276 reference proxy of crop performance was aimed at limiting the effects of outliers, that could
277 wrongly condition deductions if different choices, like mean or maximum values, were
278 considered. PR95Y were analyzed by time series decomposition. Therefore, the main
279 components, i.e. trend, seasonal, residuals were extracted (Verbesselt et al. 2010). In
280 particular, trend component was calculated from PR95Y by LOESS (Locally Estimated
281 Scatterplot Smoothing) filtering with span=0.5 (Cleveland 1979) and a first order polynomial
282 approximation. Seasonal component was modelled by Fast Fourier Transform filtering (FFT)

283 (Testa et al. 2018) applied to the previously de-trended data. Main (low) frequency
284 components were finally removed from de-trended data to obtain residuals. Trend analyses
285 graphically showed that the most of crop classes (excluded vineyards-221 and mixed
286 natural/cultivated areas-243) alternated three different behaviors (phases) in the considered
287 period, each lasting about 7 years. This time span suggests that, presently and probably, mid-
288 term algorithms for risk estimates in the agricultural context must be tuned with a time
289 horizon of 7 years. With special focus on CLC2012 class 211, corresponding to “not-irrigated
290 arable land”, and including the most important (from an economical point of view) crops in
291 the area, a numerical analysis was done to verify what graphs showed. Analysis was based on
292 a 1st derivative approach, aimed at finding the time of PR95Y maxima and minima
293 occurrences. It confirmed that one minimum took place in 2007 and two maxima in 2000 and
294 2014, respectively.

295 PR95Y crop classes were consequently split into 3 phases and each of them modelled
296 by a 1st order polynomial that proved to well fit observations (see table 6 in Result and
297 Discussion section). Each model, has to be interpreted as the basis to operate risk estimation
298 in the considered period, with the hypothesis that higher the NDVI, lower the associated risk
299 for yield reduction.

300 Significance of changes occurred along the modelled trends was tested by comparing
301 theoretical accuracy of NDVI measures (0.02, Borgogno, Lessio, and Gomarasca 2016) with
302 NDVI differences recorded between the start and the end of the considered phase (table 6 in
303 Results Section).

304 It was found that exactly class 211, showed the most significant NDVI total variation
305 within all the recognized behavioral phases. Consequently, successive analysis aimed at
306 locally and yearly tuning the model was focused only on class 211.

307 Modelled trends of PR95Y were translated into the correspondent (possible) insurance
308 meaning by defining the following risk rate correction factor (hereinafter called "discount",
309 $d(t)$):

$$310 \quad d(t) = \left(\frac{\gamma + \delta}{\gamma \cdot t + \delta} \right) \cdot 100 \quad (1)$$

311 where γ (gain) and δ (offset) are the trend line coefficients (estimated by ordinary least square
312 OLS); t is the counter of the years passed from the first one (basis year) involved in the
313 considered phase.

314 If $d(l) > 100$ (NDVI value at the l year $<$ NDVI value at the 1st year) the insurance premium
315 should be proportionally increased in respect of the basis year; if instead the value of $d(l) <$
316 100 the insurance premium should be proportionally decreased in respect of the basis year.

317 As far as the S2 data are concerned, they were used to spatially and yearly tune average class
318 trends modelled with respect to MODIS data. The obtained (macro-) class discount rate was
319 then refined considering the local conditions where a crop field is located in. Firstly, the 211
320 CLC2012 class was decomposed, where possible, into the main crops that reasonably could
321 be aggregated in the same CLC codification: wheat, corn, ryegrass and meadow. Class 211
322 disaggregation was achieved georeferenced farmers' declarations (containing crop type
323 description) for CAP purposes by joining the available cadastral parcels map with the
324 correspondent tabular data. The proposed procedure is based on local NDVI anomaly
325 computation (eq.2), defined as the ratio between the local (averaged at field level) 95th
326 percentile of the NDVI annual profile and the one averaged over the whole considered class
327 (wheat, corn, ryegrass and meadow).

$$328 \quad z_i(x, y, t) = \frac{\mu_i(x, y, t)}{\mu_{c_j}(t)} \quad (2)$$

329 where $\mu_i(x, y, t)$ is the 95th percentile of the local NDVI values (averaged over a parcel) of the
330 i -th parcel and $\mu_{c_j}(t)$ the 95th percentile of the entire class NDVI values at the t year.

331 It is worth to stress that $\mu_i(x,y,t)$ has to be computed from the same dataset that $\mu_{c_j}(t)$ is
332 computed from, i.e. S2_TS. With this premise, a new correction factor $k(x,y,t)$ timely and
333 spatially varying, see eq. 3, can be computed for each cadastral parcel and year to update
334 insurance premium/fee.

$$335 \quad k(x,y,t) = d(t) \cdot \frac{1}{Z_{pi}(x,y,t)} \quad (3)$$

336 where $d(t)$ is the discount rate for the generic t year after the first one of the new modelled
337 trend and $1/Z_{pi}$ is the local and annual tuning coefficient of eq. 2. Parcels with a $Z_{pi}>1$ behave
338 better than the correspondent class average and, consequently, the related annual insurance
339 premium is expected to be lower, being the parcel unlikely to be the object of a disaster. Vice
340 versa if $Z_{pi}<1$. If the applied insurance fee at the starting year of the new trend is known (P_{1st})
341 the updated one at the generic t year after the first one is (eq. 4).

$$342 \quad P(x,y,t) = P_{1st}(x,y,t) \cdot k(x,y,t) \quad (4)$$

343 With respect to the above mentioned operational steps, a map of $k(x,y,t)$ factor was generated
344 for both 2016 and 2017 years taking care, separately, of the specific statistics of the
345 considered classes. Procedure workflow is reported in the graph of fig. 2.

346 [FIGURE 2]

347 **Results and discussion**

348 The first analysis was aimed at characterizing main land use classes in the study area
349 with reference to the CLC2012 Level 1 codification. It resulted that the 35% of the Piemonte
350 region is specifically devoted to agriculture, making the area a good benchmark for testing
351 new insurance strategies in the agricultural field (table 5).

352 [TABLE 5]

353 In the first part of the work, aimed at testing and modelling mid-term trends of crops, all the
354 CLC2012 Level 3 classes of table 4 were considered. MOD_TS was used to model mid-term
355 trends of vegetation with reference to the annual 95th percentile averaged at class level. Class

356 NDVI profiles (PR95Y) were analyzed by time decomposition separating trends from
357 seasonality by decomposition approach. It was found that, for the investigated crop classes,
358 PR95Y could be generally split into 3 phases, that were singularly modelled by a 1st order
359 polynomial (figure 3). Obtained values of unitary variation of NDVI (gain of the trend line)
360 and the correspondent coefficients of determination (R^2) are reported in table 6, together with
361 the total NDVI variation within the modelled period.

362 [FIGURE 3]

363 [TABLE 6]

364 Gain values and total NDVI variations were compared with the theoretical NDVI accuracy
365 (0.02) to test “operational” significance of changes. Given the economic impact of class 211
366 (Not-irrigated arable land) in the area, this solely was selected for the successive modelling
367 steps, disaggregating it into the main included crop types (wheat, corn, meadow, ryegrass).
368 According to table 6 class 211 showed the most significant variation of NDVI trend for all the
369 recognized phases (2000-2007, 2007-2014, 2014-2018).

370 The proposed 1st order polynomial model, has consequently to be used to estimate insurance
371 risk trend for those crops belonging to the CLC2012 211 class, with the hypothesis that higher
372 the NDVI, lower the associated risk for yield reduction. Trend defines a general behavior of
373 class 211 in the whole considered region, with no matter about specific site features, yearly
374 meteorological conditions, crop types and crop management practices. Consequently, to
375 refine the risk estimate given by the model, a further analysis is required at field level aimed
376 at qualifying performances of crops (in terms of NDVI value), with reference to their type (as
377 declared by farmers and recorded within PAC declarations). Performance can be evaluated in
378 a relative way by class-specific anomaly computation operated at field level (eq. 2). To
379 exemplify this operation, two maps of NDVI anomaly (2016 and 2017) were generated for the
380 area with respect to the available S2_TS. Anomaly was separately computed and mapped for

381 the four considered crop types and then mosaicked to generate a single map (figure 4) useful
382 for operational purposes.

383 [FIGURE 4]

384 Some statistics describing crop type anomalies in 2016 and 2017 were computed and
385 compared trying to emphasize dynamicity of the phenomenon. Three anomaly classes were
386 considered: class 1: $z_i(x, y, t) < 0.95$; class 2: $0.95 < z_i(x, y, t) < 1.05$; class 3: $z_i(x, y, t) > 1.05$
387 Results are reported in Tab.7.

388 [TABLE 7]

389 Results show that, in spite of the reduced size of the study area, differences between 2016 and
390 2017 were not negligible as their differences, reported in table 8, demonstrate.

391

392 [TABLE 8]

393 This fact suggests that agriculture landscape is dynamic and constantly changes in
394 class distribution and performance depending on the considered year. Consequently, robust
395 and reliable ground data would be required to, correctly, locate crops and making possible
396 reasonable interpretations of ongoing processes and anomalies. It is, rarely, possible to,
397 rigorously, compare different years and giving a single interpretation of detected anomalies,
398 since too many variables interact, related to climate/weather, crop rotation, agronomic
399 practices, soil nutrient content, etc. Nevertheless, the proposed procedure permits to map
400 anomalies, i.e the final effect of all the acting agents, supplying a new spatially based support
401 for calibrating and addressing new insurance strategies with the aim of tuning the risk
402 associated with a certain crop in a certain area. This can be obtained translating the anomaly
403 map into the correspondent $k(x,y,t)$ factor map. Again, this was done for both the 2016 and
404 2017 years with reference to the 4 investigated crops (figure 5).

405 [FIGURE 5]

406 $k(x,y,t)$ is a map specifically describing the spatial distribution of the updating factor to
407 use for tuning the insurance premium for that type of crop at that position in that year,
408 assuming, as basis, the premium paid in the first year of the ongoing modelled trend.

409 The proposed methodology tries to face some of the challenges proposed by the
410 review of De Leeuw et al. (De Leeuw et al. 2014) about features that insurance companies
411 require to remote sensing based approaches in the agricultural context. One of them is the
412 need of timely and spatially comparable, crop type specific metrics available with a
413 sufficiently high temporal resolution. NDVI time series from MODIS and S2 dataset well fit
414 these requirements. Additionally, the proposed procedure falls within the general logic of the
415 “index based” crop insurance policies as proposed by different authors (Rao 2010; Bokusheva
416 et al. 2012; Bobojonov, Aw-Hassan, and Sommer 2014). It sounds similar to those reported
417 by many authors (Patankar 2011; Makaudze and Miranda 2010; Turvey and McLaurin 2012),
418 but the main difference relies in the joint adoption of the following steps. With reference to
419 MODIS-based trend analysis, we preventively synthesized yearly spectral information in a
420 single metric (PR95Y); secondly, a time series decomposition of PR95Y was achieved to
421 extract the average trends (low frequency variations) in the period 2000-2018; finally, a break
422 point investigation was performed to look for trend phases along the explored period.

423 The adoption of PR95Y as synthetic metric was intended to limit noise effects given
424 by NDVI values related to those annual periods when vegetation is not active. This can
425 somehow limit time series decomposition (Forkel et al. 2013). Conversely, a properly
426 designed metric can drive to a more robust estimate of the inter-annual behavior of vegetation
427 (Zhou et al. 2016; Hird and McDermid 2009). It is worth to remind that common approaches
428 for time series decomposition like BFAST (Breaks For Additive Season and Trend) (Fang et
429 al. 2018) and STL (Seasonal decomposition of Time Series by Loess) (Lu et al. 2003),
430 generally, process the entire multi-annual time series with no a-priori synthesis.

431 Ordinary long-term trend modelling only show the overall trend along the entire analyzed
432 period, with no interest about possible existing sub-periods. These can be significant and,
433 consequently, important to be recognized to get indications about the average time persistence
434 of a certain trend and to better calibrate models that are expected to have economic impacts. A
435 break point analysis was, therefore, achieved looking for changes in PR95Y trend derivative
436 sign (Schucknecht et al. 2013; de Jong et al. 2012). Three sub-period trends were found, for
437 the most of the analyzed CLC classes. Future developments could be addressed to improve
438 break point detection using algorithms like DBEST (Detecting Breakpoints and Estimating
439 Segments in Trend) proposed by (Jamali et al. 2015; Forkel et al. 2013).

440 As far as anomaly mapping is concerned a similar approach was found in a recent paper by
441 Shirsath et al. (Shirsath, Sehgal, and Aggarwal 2020), while specific applications in the
442 agricultural insurance sector are reported in Lekakis et al. (2020).

443 Our expectation is that the proposed procedure, based on freely available dataset and
444 simple data processing, could support insurance companies to monitor crops behavior at the
445 mid and short term, making possible to, somehow, map the probability of finding a favorable
446 or unfavorable trend for a specific crop. This is a basic condition for consciously calibrating
447 insurance fees. In favorable areas, showing an increasing trend in biomass production, a lower
448 annual crop premium could be defined, encouraging farmers to take out insurance.
449 Expectation is that higher the number of insured farmers, lower the insurance fees;
450 consequently, it is our conviction that this approach could drive faster the ongoing process of
451 making farmers closer to insurance. The proposed method can be certainly applied in other
452 regions, but some key concepts must be considered. Firstly, persistent cloud cover can affect
453 results especially in early phenological stages (e.g. emergence, tillering). Secondly,
454 comparison is reliable only if explored fields fall in the same “agronomic region”, where both
455 climate and management system are sufficiently homogeneous.

457 Conclusions

458 This research was stimulated by technicians of the Piemonte Region administration
459 with the aim of finding new ways to monitor crops in such a way to make more attractive (for
460 farmers) insurance policies covering yields loss. Attraction depends on the possibility of
461 convincing farmers of the need of an insurance covering and on the opportunity, for insurance
462 company, of better calibrate (possibly reduce) fees to apply to farmers. Consequently, this
463 work was addressed to develop and propose a methodological approach aimed at supporting
464 agriculture-devoted insurance strategies based on time series of free multispectral satellite
465 data. The basic idea was to relate crop performances at the mid and short term to calibrate
466 insurance fees, taking care about both time trend and spatial distribution of biomass
467 production by crops. A study area was selected within the Piemonte Region (NW Italy) to act
468 as paradigm for testing and presenting the methodology. According to obtained results these
469 considerations can be done: a) MOD13Q1 product, supplying 16 days composite NDVI maps
470 with a geometric resolution of 250 m and ranging from 2000 up to 2018, proved to be
471 effective in describing mid-term trends of crop performance at both regional and agriculture
472 macro-class level; b) NDVI map time series obtained from Copernicus Sentinel 2 data, having
473 a higher geometric resolution (10 m), permitted to detail investigation at field level, making
474 possible to refine insurance risk estimate and linking it to the local specific condition of crops.
475 Refinement was obtained with reference to the local anomaly concept computed around the
476 crop class average value. With respect to the above mentioned criteria, a simple but extremely
477 operational mathematical model was suggested to calibrate insurance fee at year and field
478 level. During the tests an evidence was found concerning duration of growing (or decreasing)
479 trends of crop performances in the area. In fact, a 7 year lasting period was recognized by
480 time series decomposition of NDVI maps time series from MOD13Q1 product, suggesting

481 that a new mathematical model have to be possibly calibrated after 7 years from the starting
482 date of the previously adopted one. Eventual further improvements of the proposed method
483 can be certainly possible especially if a new approach will be applied in ground data
484 supplying. A constant, reliable and spatially distributed flux of information from farmers to
485 the system is desirable to continuously monitoring the numerous varying variables that
486 determine anomaly occurrences. This strategy could drive to propose new insurance indexed
487 policies for protecting the whole agricultural sector in view of the effects of climate change.
488 More appropriate insurance contracts can be proposed to farmers and encourage him to make
489 use of this type of cover for its activity. In other words, insurance company can attract new
490 customers and farmers can protect themselves with reasonable and demonstrable prices.

491 Aside the main purpose this methodology was developed for, it is expected that it
492 could also represent a valuable tool for investigating vast areas with the aim of recognizing
493 ongoing anomalies in crops behavior: it would offer an efficient, economically competitive
494 and immediate control or service. It is worth to remind that the proposed approach highly
495 relies on accurate field controls that should report type and time of crucial events and crop
496 management activities, that can supply the right interpretation keys of the observed and
497 mapped phenomena.

498 **Acknowledgments**

499 We would like to thank Germano Tosin, Emanuele Possiedi and Dario Airaudo,
500 technicians by the Piemonte regional administration – Agriculture Sector, for having provided
501 guidelines and fundamental operational information useful to reach the results presented in
502 this work.

503 **References**

504 Atzberger, C. 2013. “Advances in remote sensing of agriculture: Context description, existing
505 operational monitoring systems and major information needs”. *Remote sensing*. 5.2: 949-981.

- 506 Baas, S., M. Trujillo, and N. Lombardi. 2015. "Impact of disasters on agriculture and food security".
507 FAO.
- 508 Barnes, W. L., Pagano, T. S., & Salomonson, V. V. 1998. "Prelaunch characteristics of the moderate
509 resolution imaging spectroradiometer (MODIS) on EOS-AM1". *IEEE Transactions on*
510 *Geoscience and Remote Sensing*. 36.4: 1088-1100.
- 511 Bastiaanssen, W. G., Molden, D. J., & Makin, I. W. 2000. "Remote sensing for irrigated agriculture:
512 examples from research and possible applications". *Agricultural water management*. 46.2:
513 137-155.
- 514 Beerli, O., & Peled, A. 2006. "Spectral indices for precise agriculture monitoring". *International*
515 *Journal of Remote Sensing*. 27.10: 2039-2047.
- 516 Bobojonov, Ihtiyor, Aden Aw-Hassan, and Rolf Sommer. 2014. "Index-Based Insurance for Climate
517 Risk Management and Rural Development in Syria." *Climate and Development* 6 (2). Taylor
518 & Francis: 166–178.
- 519 Bokusheva, Raushan, L. Spivak, Irina Vitkovskaya, F. Kogan, and Madina Batyrbayeva. 2012.
520 "Application of Remote-Sensing Data in the Index-Based Insurance Design." In *2012 IEEE*
521 *International Geoscience and Remote Sensing Symposium*, 5311–5314. IEEE.
- 522 Borgogno-Mondino, Enrico, Andrea Lessio, and Mario Angelo Gomasasca. 2016. "A fast operative
523 method for NDVI uncertainty estimation and its role in vegetation analysis." *European*
524 *Journal of Remote Sensing* 49.1: 137-156.
- 525 Borgogno Mondino, E., and M. Gajetti. 2017. "Preliminary considerations about costs and potential
526 market of remote sensing from UAV in the Italian viticulture context." *European Journal of*
527 *Remote Sensing* 50.1: 310-319.
- 528 Borgogno-Mondino, Enrico, Filippo Sarvia, and Mario A. Gomasasca. 2019. "Supporting Insurance
529 Strategies in Agriculture by Remote Sensing: A Possible Approach at Regional Level."
530 *International Conference on Computational Science and Its Applications*. Springer, Cham.
- 531 Borriello, Raffaele. 2003. "Assicurazioni, gestione dei rischi in agricoltura e garanzia dei redditi."
532 *Convegno Ismea, Roma* 25.
- 533 Büttner, G. 2014. "CORINE land cover and land cover change products. In Land use and land cover
534 mapping in Europe." Springer, Dordrecht: 55–74.
- 535 Chen, P. Y., Fedosejevs, G., Tiscareno-Lopez, M., & Arnold, J. G. 2006. "Assessment of MODIS-
536 EVI, MODIS-NDVI and VEGETATION-NDVI composite data using agricultural
537 measurements: An example at corn fields in western Mexico". *Environmental monitoring and*
538 *assessment*. 119.1-3: 69-82.
- 539 Chenet, Hugues. 2019. "Climate change and financial risk." *Available at SSRN 3407940*.
- 540 Chmielewski, Frank-M., Antje Müller, and Ekko Bruns. 2004. "Climate changes and trends in
541 phenology of fruit trees and field crops in Germany, 1961–2000." *Agricultural and Forest*
542 *Meteorology* 121.1-2: 69-78.

- 543 Cleveland, William S. 1979. "Robust Locally Weighted Regression and Smoothing Scatterplots."
544 *Journal of the American Statistical Association* 74 (368). Taylor & Francis: 829–836.
- 545 Colwell, H., Carneggie, D., Croxton, R., Manzer, F., Simonett, D., & Steiner, D. 1970. "Applications
546 of remote sensing in agriculture and forestry". *Applications of remote sensing in agriculture
547 and forestry*.
- 548 Conforti, P., S. Ahmed, and G. Markova. 2018. "Impact of disasters and crises on agriculture and food
549 security, 2017."
- 550 de Jong, Rogier, Jan Verbesselt, Michael E. Schaepman, and Sytze De Bruin. 2012. "Trend Changes
551 in Global Greening and Browning: Contribution of Short-Term Trends to Longer-Term
552 Change." *Global Change Biology* 18 (2). Wiley Online Library: 642–655.
- 553 De Leeuw, Jan, Anton Vrieling, Apurba Shee, Clement Atzberger, Kiros M. Hadgu, Chandrashekhar
554 M. Biradar, Humphrey Keah, and Calum Turvey. 2014. "The Potential and Uptake of Remote
555 Sensing in Insurance: A Review." *Remote Sensing* 6 (11). Multidisciplinary Digital Publishing
556 Institute: 10888–10912.
- 557 De Ruvo E., Giuliani F., Lasorsa N., Pennucci M., Rosatelli L. 2019. "Rapporto sulla gestione del
558 rischio in agricoltura 2019". *ISMEA - Istituto di Servizi per il Mercato Agricolo Alimentare*.
- 559 Didan, K. 2015. "MOD13Q1 MODIS/Terra vegetation indices 16-day L3 global 250m SIN grid
560 V006". *NASA EOSDIS Land Processes DAAC*.
- 561 Drusch, M., Del Bello, U., Carlier, S., Colin, O., Fernandez, V., Gascon, F., ... & Meygret, A. 2012.
562 "Sentinel-2: ESA's optical high-resolution mission for GMES operational services". *Remote
563 sensing of Environment*. 120: 25-36.
- 564 Easterling, D. R., Meehl, G. A., Parmesan, C., Changnon, S. A., Karl, T. R., & Mearns, L. O. 2000.
565 "Climate extremes: observations, modeling, and impacts". *Science*, 289.5487: 2068-2074.
- 566 Estrela, M. J., D. Peñarrocha, and M. Millán. 2000. "Multi-annual drought episodes in the
567 Mediterranean (Valencia region) from 1950–1996. A spatio-temporal analysis." *International
568 Journal of Climatology: A Journal of the Royal Meteorological Society* 20.13: 1599-1618.
- 569 Fang, Xiuqin, Qiuhan Zhu, Liliang Ren, Huai Chen, Kai Wang, and Changhui Peng. 2018. "Large-
570 Scale Detection of Vegetation Dynamics and Their Potential Drivers Using MODIS Images
571 and BFAST: A Case Study in Quebec, Canada." *Remote Sensing of Environment* 206.
572 Elsevier: 391–402.
- 573 Feranec, J., Soukup, T., Hazeu, G., & Jaffrain, G. (Eds.). 2016. "European landscape dynamics:
574 CORINE land cover data". *CRC Press*.
- 575 Forkel, Matthias, Nuno Carvalhais, Jan Verbesselt, Miguel D. Mahecha, Christopher SR Neigh, and
576 Markus Reichstein. 2013. "Trend Change Detection in NDVI Time Series: Effects of Inter-
577 Annual Variability and Methodology." *Remote Sensing* 5 (5). Multidisciplinary Digital
578 Publishing Institute: 2113–2144.
- 579 Food and Agriculture Organization (FAO). 2007. "Adaptation to Climate Change in Agriculture,
580 Forestry and Fisheries: Perspective, Framework and Priorities."

- 581 Grillakis, Manolis G. 2019. "Increase in severe and extreme soil moisture droughts for Europe under
582 climate change." *Science of The Total Environment* 660: 1245-1255.
- 583 Haghverdi, Amir, Robert A. Washington-Allen, and Brian G. Leib. 2018. "Prediction of cotton lint
584 yield from phenology of crop indices using artificial neural networks." *Computers and
585 Electronics in Agriculture* 152: 186-197.
- 586 Hay, Fiona. 2019. "Seed Banking as Future Insurance Against Crop Collapses." *Oxford Research
587 Encyclopedia of Environmental Science*.
- 588 Hird, Jennifer N., and Gregory J. McDermid. 2009. "Noise Reduction of NDVI Time Series: An
589 Empirical Comparison of Selected Techniques." *Remote Sensing of Environment* 113 (1).
590 Elsevier: 248–258.
- 591 Islam, M. B., Becker, M., Bargiel, D., Ahmed, K. R., Duzak, P., & Eman, N. G. 2017. "Sentinel-2
592 Satellite Imagery based Population Estimation Strategies at FabSpace 2.0 Lab Darmstadt". In
593 *CLEF (Working Notes)*.
- 594 Jamali, Sadegh, Per Jönsson, Lars Eklundh, Jonas Ardö, and Jonathan Seaquist. 2015. "Detecting
595 Changes in Vegetation Trends Using Time Series Segmentation." *Remote Sensing of
596 Environment* 156. Elsevier: 182–195.
- 597 Jensen, N., Stoeffler, Q., Fava, F., Vrieling, A., Atzberger, C., Meroni, M., ... & Carter, M. 2019.
598 "Does the design matter? Comparing satellite-based indices for insuring pastoralists against
599 drought". *Ecological economics* 162: 59-73.
- 600 Jonsson, Per, and Lars Eklundh. 2002. "Seasonality extraction by function fitting to time-series of
601 satellite sensor data." *IEEE transactions on Geoscience and Remote Sensing* 40.8 (2002):
602 1824-1832.
- 603 Lekakis, Emmanuel, Stylianos Kotsopoulos, Gregory Mygdakos, Agathoklis Dimitrakos, Ifigenia-
604 Maria Tsioutsia, and Polimachi Simeonidou. 2020. "Redefining Agricultural Insurance
605 Services Using Earth Observation Data. The Case of Beacon Project." In *International
606 Symposium on Environmental Software Systems*, 90–101. Springer.
- 607 Leprieur, Catherine, Michel M. Verstraete, and Bernard Pinty. 1994. "Evaluation of the performance
608 of various vegetation indices to retrieve vegetation cover from AVHRR data." *Remote Sensing
609 Reviews* 10.4: 265-284.
- 610 Lobell, David B., and Gregory P. Asner. 2003. "Climate and management contributions to recent
611 trends in US agricultural yields." *Science* 299.5609: 1032-1032.
- 612 Lu, Hua, Michael R. Raupach, Tim R. McVicar, and Damian J. Barrett. 2003. "Decomposition of
613 Vegetation Cover into Woody and Herbaceous Components Using AVHRR NDVI Time
614 Series." *Remote Sensing of Environment* 86 (1): 1–18.
- 615 Lu, Junyu, Gregory J. Carbone, and Peng Gao. 2019. "Mapping the agricultural drought based on the
616 long-term AVHRR NDVI and North American Regional Reanalysis (NARR) in the United
617 States, 1981–2013." *Applied geography* 104: 10-20.

- 618 Makaudze, Ephias M., and Mario J. Miranda. 2010. "Catastrophic Drought Insurance Based on the
619 Remotely Sensed Normalised Difference Vegetation Index for Smallholder Farmers in
620 Zimbabwe." *Agrekon* 49 (4). Taylor & Francis: 418-432.
- 621 Mavromatis, T. "Drought index evaluation for assessing future wheat production in Greece. 2007. "
622 *International Journal of Climatology: A Journal of the Royal Meteorological Society* 27.7:
623 911-924.
- 624 Min, S. K., Kwon, W. T., Park, E. H., & Choi, Y. 2003. "Spatial and temporal comparisons of
625 droughts over Korea with East Asia". *International Journal of Climatology: A Journal of the
626 Royal Meteorological Society* 23.2: 223-233.
- 627 Meir, Patrick, Peter Cox, and John Grace. 2006. "The influence of terrestrial ecosystems on climate."
628 *Trends in Ecology & Evolution* 21.5: 254-260.
- 629 Modarres, Reza. 2007. "Streamflow drought time series forecasting." *Stochastic Environmental
630 Research and Risk Assessment* 21.3: 223-233.
- 631 Nanzad, L., Zhang, J., Tuvdendorj, B., Nabil, M., Zhang, S., & Bai, Y. 2019. "NDVI anomaly for
632 drought monitoring and its correlation with climate factors over Mongolia from 2000 to
633 2016". *Journal of arid environments* 164: 69-77.
- 634 Patankar, Mangesh. 2011. "Comprehensive Risk Cover through Remote Sensing Techniques in
635 Agriculture Insurance for Developing Countries: A Pilot Project." *ILO Microinsurance
636 Innovation Facility Research Paper*, no. 6.
- 637 Potop, Vera. 2011. "Evolution of drought severity and its impact on corn in the Republic of Moldova."
638 *Theoretical and Applied Climatology* 105.3-4: 469-483.
- 639 Quiring, Steven M., and Timothy N. Papakryiakou. 2003. "An evaluation of agricultural drought
640 indices for the Canadian prairies." *Agricultural and forest meteorology* 118.1-2: 49-62.
- 641 Rao, Kolli N. 2010. "Index Based Crop Insurance." *Agriculture and Agricultural Science Procedia* 1.
642 Elsevier: 193-203.
- 643 Rhee, J., Im, J., & Carbone, G. J. 2010. "Monitoring agricultural drought for arid and humid regions
644 using multi-sensor remote sensing data". *Remote Sensing of Environment*. 114.12: 2875-2887.
- 645 Rojas, O., Vrieling, A., & Rembold, F. 2011. "Assessing drought probability for agricultural areas in
646 Africa with coarse resolution remote sensing imagery". *Remote sensing of Environment*.
647 115.2: 343-352.
- 648 Rouse Jr, J. W., Haas, R. H., Deering, D. W., Schell, J. A., & Harlan, J. C. 1974. "Monitoring the
649 Vernal Advancement and Retrogradation (Green Wave Effect) of Natural Vegetation". *Great
650 Plains Corridor*.
- 651 Sahoo, R. N., Ray, S. S., & Manjunath, K. R. 2015. "Hyperspectral remote sensing of
652 agriculture". *Current Science*. 848-859.
- 653 Sánchez, N., González-Zamora, Á., Martínez-Fernández, J., Piles, M., & Pablos, M. 2018. "Integrated
654 remote sensing approach to global agricultural drought monitoring". *Agricultural and Forest
655 Meteorology*, 259: 141-153.

- 656 Sandholt, I., Nyborg, L., Fog, B., Lô, M., Bocoum, O., & Rasmussen, K. 2003. "Remote sensing
657 techniques for flood monitoring in the Senegal River Valley". *Geografisk Tidsskrift-Danish*
658 *Journal of Geography*. 103.1: 71-81.
- 659 Sanyal, J., & Lu, X. X. 2004. "Application of remote sensing in flood management with special
660 reference to monsoon Asia: a review". *Natural Hazards*. 33.2: 283-301.
- 661 Sarvia, F., S. De Petris, and E. Borgogno-Mondino. 2019. "Remotely sensed data to support insurance
662 strategies in agriculture." *Remote Sensing for Agriculture, Ecosystems, and Hydrology XXI*.
663 Vol. 11149. International Society for Optics and Photonics.
- 664 Schucknecht, Anne, Stefan Erasmi, Irmgard Niemeyer, and Jörg Matschullat. 2013. "Assessing
665 Vegetation Variability and Trends in North-Eastern Brazil Using AVHRR and MODIS NDVI
666 Time Series." *European Journal of Remote Sensing* 46 (1). Taylor & Francis: 40–59.
- 667 Sentinel, E. S. A. (2). User Handbook. 2015.
- 668 Severini, S., Biagini, L., & Finger, R. 2019. "Modeling agricultural risk management policies–The
669 implementation of the Income Stabilization Tool in Italy". *Journal of Policy Modeling*. 41.1:
670 140-155.
- 671 Shanmugapriya, P., Rathika, S., Ramesh, T., & Janaki, P. 2019. "Applications of Remote Sensing in
672 Agriculture. A Review". *Int. J. Curr. Microbiol. Appl. Sci.* 8: 2270-2283.
- 673 Shirsath, Paresh B., Vinay Kumar Sehgal, and Pramod K. Aggarwal. 2020. "Downscaling Regional
674 Crop Yields to Local Scale Using Remote Sensing." *Agriculture* 10 (3). Multidisciplinary
675 Digital Publishing Institute: 58.
- 676 Silleos, N., Perakis, K., & Petsanis, G. 2002. "Assessment of crop damage using space remote sensing
677 and GIS". *International Journal of Remote Sensing*. 23.3: 417-427.
- 678 Solano, R., Didan, K., Jacobson, A., & Huete, A. 2010. "MODIS vegetation index user's guide
679 (MOD13 series)". *Vegetation Index and Phenology Lab, The University of Arizona*, 1-38.
- 680 Son, N. T., Chen, C. F., Chen, C. R., Minh, V. Q., & Trung, N. H. 2014. "A comparative analysis of
681 multitemporal MODIS EVI and NDVI data for large-scale rice yield estimation". *Agricultural*
682 *and forest meteorology*. 197: 52-64.
- 683 Steven, M. D., and Clark, J. A. 2013. "Applications of remote sensing in agriculture". *Elsevier*.
- 684 Weiss, M., Jacob, F., and Duveiller, G. 2020. "Remote sensing for agricultural applications: A meta-
685 review". *Remote Sensing of Environment*. 236. 111402.
- 686 White, Gilbert F. 1994. "A perspective on reducing losses from natural hazards." *Bulletin of the*
687 *American Meteorological Society* 75.7: 1237-1240.
- 688 Wilhite D. A., 1993. "Drought Assessment, Management and Planning: Theory and Case Studies".
689 *Kluwer Academic Publisher's*. 293.
- 690 Wilhite, Donald A., 2012. "Drought assessment, management, and planning: theory and case studies:
691 theory and case studies". Vol. 2. *Springer Science & Business Media*.

- 692 Tao, F., Yokozawa, M., Liu, J., & Zhang, Z. 2008. "Climate–crop yield relationships at provincial
693 scales in China and the impacts of recent climate trends". *Climate Research*, 38.1: 83-94.
- 694 Testa, Stefano, K. Soudani, Luigi Boschetti, and E. Borgogno Mondino. 2018. "MODIS-Derived EVI,
695 NDVI and WDRVI Time Series to Estimate Phenological Metrics in French Deciduous
696 Forests." *International Journal of Applied Earth Observation and Geoinformation* 64: 132–
697 144.
- 698 Turvey, Calum G., and Megan K. Mclaurin. 2012. "Applicability of the Normalized Difference
699 Vegetation Index (NDVI) in Index-Based Crop Insurance Design." *Weather, Climate, and
700 Society* 4 (4): 271–284.
- 701 Verbesselt, J., Hyndman, R., Newnham, G., & Culvenor, D. 2010. "Detecting trend and seasonal
702 changes in satellite image time series". *Remote sensing of Environment*. 114.1: 106-115.
- 703 Zambrano, F., Vrieling, A., Nelson, A., Meroni, M., & Tadesse, T. 2018. "Prediction of drought-
704 induced reduction of agricultural productivity in Chile from MODIS, rainfall estimates, and
705 climate oscillation indices". *Remote sensing of environment*, 219: 15-30.
- 706 Zhang, F., Chen, Y., Zhang, J., Guo, E., Wang, R., & Li, D. 2019. "Dynamic drought risk assessment
707 for maize based on crop simulation model and multi-source drought indices". *Journal of
708 cleaner production*, 233: 100-114.
- 709 Zhang, X., Zhang, B., Wei, Z., Chen, Z. C., & Zheng, L. F. 2005. "Study on spectral indices of
710 MODIS for wheat growth monitoring". *J. Image Graphics*. 10.4: 420-424.
- 711 Zhou, Jihua, Wentao Cai, Yue Qin, Liming Lai, Tianyu Guan, Xiaolong Zhang, Lianhe Jiang, Hui Du,
712 Dawen Yang, and Zhentao Cong. 2016. "Alpine Vegetation Phenology Dynamic over 16
713 Years and Its Covariation with Climate in a Semi-Arid Region of China." *Science of the Total
714 Environment* 572. Elsevier: 119–128.

715 Table 1. Spatial size of the main crop types present in the study area.

Crop type	Total Area (ha)	Total Cultivated Area (ha)	Crop Area (ha)	Crop Area (%)
Ryegrass			1769	8.4%
Corn	43720	21063	7403	35.2%
Wheat			3248	15.3%
Meadow			8643	41.1%

716

717 Table 2. Technical specifications of TERRA MODIS and S2 MSI sensors as reported in
718 Barnes, Pagano, and Salomonson (1998) and Drush et al. (2012).

	MODIS	S2
Launch date	18/12/1999	23/06/2015
Orbit Altitude	705 km	786 km
Geometric resolution	b1-b3, b7: 250m	b2-b4, b8: 10m b5-b7, b8a, b11, b12: 20m b1, b9, b10: 60m
Radiometric resolution	16 bit	12 bit
Temporal resolution	16 days	10 days (5 days with S2 A/B satellites)

719

720 Table 3. Technical features of CLC2012 product as reported in Feranec et al. 2016.

	Value
Satellite data source	IRS P6 LISS III and RapidEye
Time consistency (years)	2011-2012
Geometric Accuracy (satellite data)	≤ 25 m
Geometric Accuracy (CLC)	Better than 100 m
Thematic Accuracy	≥ 85%
Minimum Mapping Unit/width	25 ha/ 100 m
Access to the data	free
Number of countries involved	39

721

722 Table 4. Codes used in CLC2012 for qualifying agricultural classes (codes from Feranec et al.
723 2016).

Level 3 code	Class
2.1.1	Not-irrigated arable land
2.1.3	Rice fields
2.2.1	Vineyards
2.2.2	Fruit trees and berry plantations
2.3.1	Pastures
2.4.2	Complex cultivation patterns
2.4.3	Land principally occupied by agriculture, with significant areas of natural vegetation

724

725

726

727

728

729 Table 5. CLC2012 L1 classes and correspondent size within Piemonte Region.

CLC2012 L1 class	CLC2012 L1 code	Area (ha)	Area (%)
Artificial surfaces	1	109938	4
Agricultural areas	2	1253649	36
Forest and semi natural areas	3	20602216	59
Wetlands	4	-	-
Water bodies	5	30878	1
Total	-	3454681	100

730

731 Table 6. Δ_{NDVI} = values of total NDVI variation along the considered period (as resulting
732 from trend line); Gain = average yearly variation of NDVI as resulting from trend line); R^2 =
733 coefficient of determination computed for the 3 trends corresponding to the recognized
734 behavioral phases. In red, values of Δ_{NDVI} that are significant with respect to NDVI measure
735 theoretical accuracy (0.02).

736

CLC Class	2000-2007			2007-2014			2014-2018		
	Δ_{NDVI} (8 years)	Gain (NDVI/year)	R^2	Δ_{NDVI} (8 years)	Gain (NDVI/year)	R^2	Δ_{NDVI} (5 years)	Gain (NDVI/year)	R^2
211	-0.0512	-0.0064	0.8879	0.0432	0.0054	0.7939	-0.0215	-0.0043	0.8299
213	-0.0040	-0.0005	0.0804	0.0032	0.0004	0.0339	0.0020	0.0004	0.1416
221	0.0240	0.0030	0.6604	0.0152	0.0019	0.3708	0.0185	0.0037	0.8651
222	-0.0096	-0.0012	0.4832	0.0032	0.0004	0.0903	-0.0050	-0.0010	0.2266
231	-0.0232	-0.0029	0.8520	0.0264	0.0033	0.8835	-0.0020	-0.0004	0.0587
242	-0.0152	-0.0019	0.5430	0.0488	0.0061	0.8971	-0.0060	-0.0012	0.5296
243	-0.0128	-0.0016	0.5930	0.0232	0.0029	0.7854	0.0075	0.0015	0.5164

737

738

739 Table 7. Statistics describing anomaly distributions for the considered crops in the study area.

740 Frequencies are given for the following anomaly classes. Class 1: $z_i(x, y, t) < 0.95$; class 2:741 $0.95 < z_i(x, y, t) < 1.05$; class 3: $z_i(x, y, t) > 1.05$

Year	2016				2017			
	Ryegrass	Corn	Wheat	Meadow	Ryegrass	Corn	Wheat	Meadow
Class 1	12.60%	31.76%	11.64%	8.73%	14.81%	14.51%	19.58%	8.51%
Class 2	43.05%	62.40%	31.61%	32.02%	38.34%	63.98%	39.41%	20.40%
Class 3	44.35%	5.84%	56.75%	59.25%	46.85%	21.51%	41.01%	71.09%

742

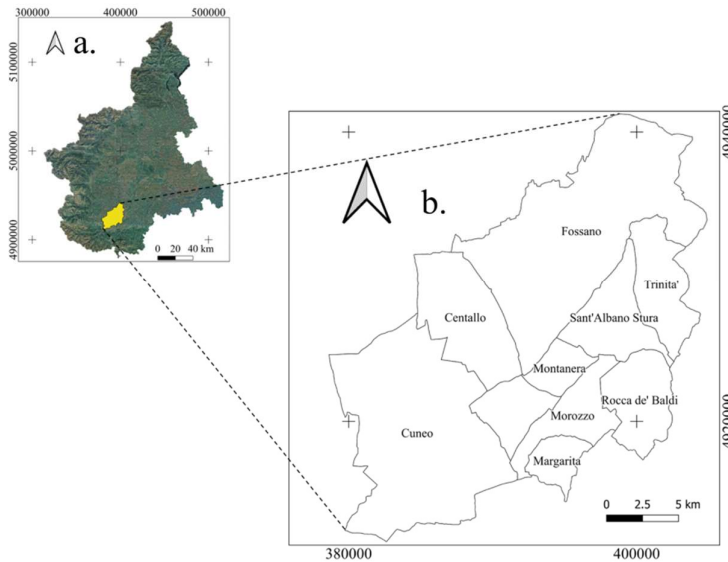
743

744 Table 8. Differences of occurrences of the above mentioned anomaly classes between 2016
745 and 2017 for the considered crops.

Anomaly 2016 - 2017				
Class	Ryegrass	Corn	Wheat	Meadow
1	2.20%	-17.24%	<u>7.93%</u>	-0.22%
2	-4.71%	1.58%	7.80%	-11.62%
3	2.50%	<u>15.67%</u>	-15.73%	<u>11.84%</u>

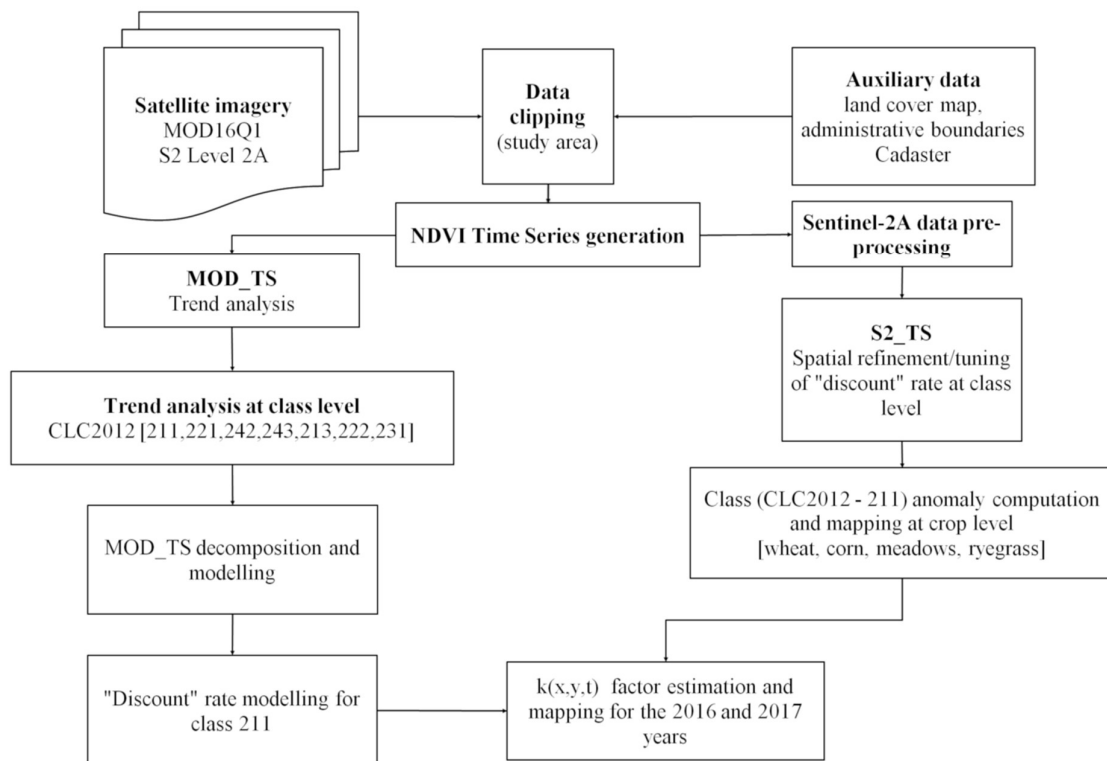
746

747 Figure 1. Study areas: a. Administrative boundaries of Piemonte Region, NW Italy. This area
 748 was assumed as the reference one for the mid-term analysis. b. Administrative boundaries of
 749 municipalities considered as focus areas for the instantaneous deductions. Their position
 750 within Piemonte Region is shown in yellow in a). Reference system is WGS 84 / UTM zone
 751 32N, EPSG: 32632.



752

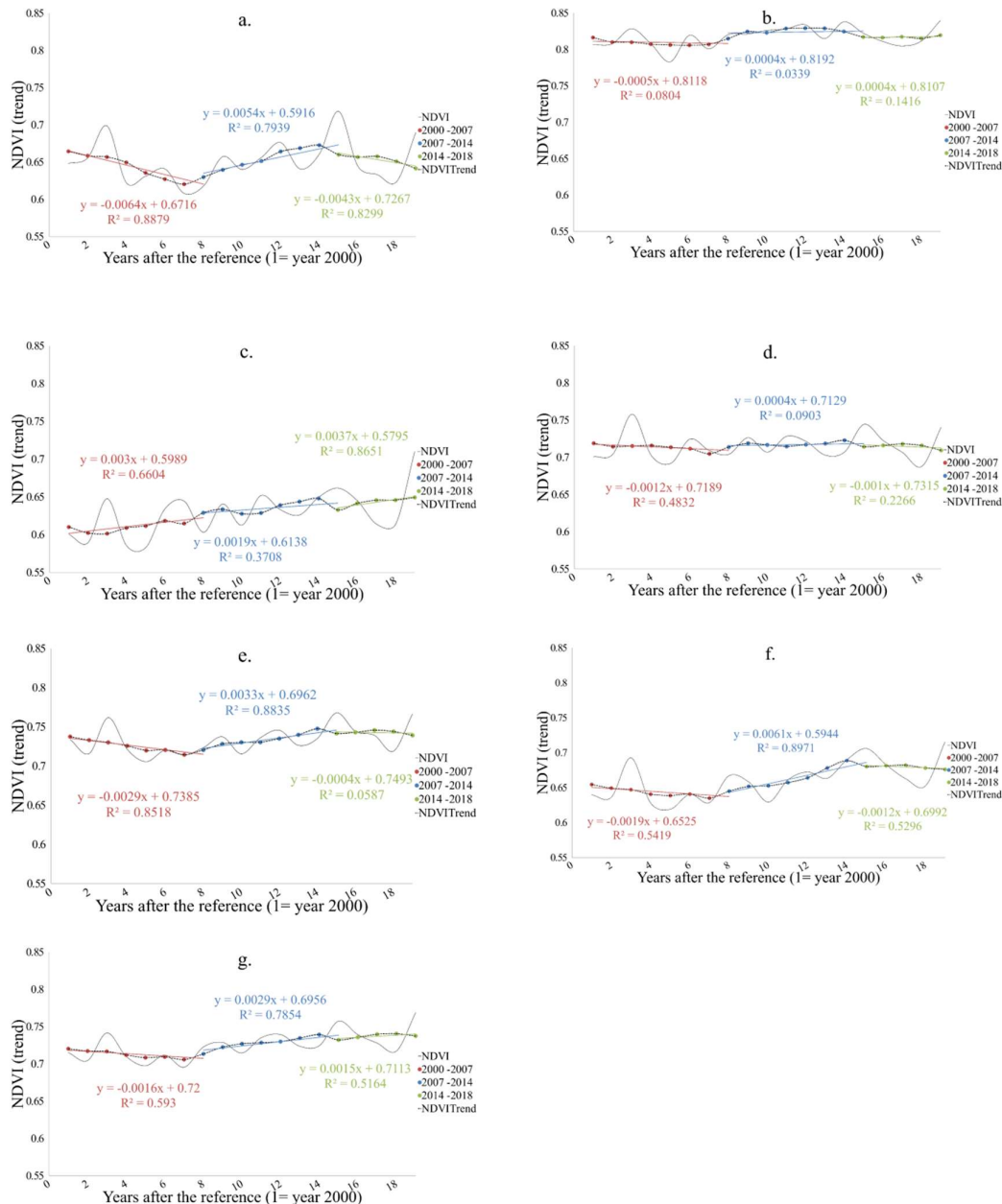
753 Figure 2. Workflow showing the main conceptual steps of the proposed methodology.



754

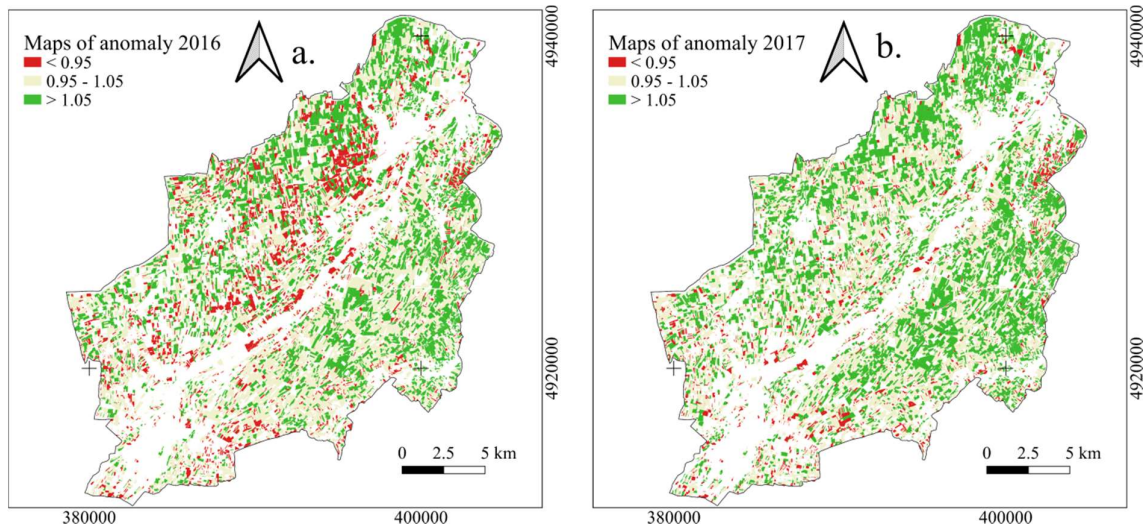
755

756 Figure 3. Temporal profiles of NDVI (PR95Y) given for all the considered agricultural
 757 classes from CLC2012-Level 3. a. Non-irrigated arable land (CLC 211); b. Rice fields (CLC
 758 213); c. Vineyards (CLC 221); d. Fruit trees and berry plantations (CLC 222); e. Pastures
 759 (CLC 231); f. Complex cultivation patterns (CLC 242); g. Land principally occupied by
 760 agriculture, with significant areas of natural vegetation (CLC 243). Graphs clearly show that
 761 three different phases characterized the period 2000-2018. They were separately modelled by
 762 a 1st order polynomial.



763
 764
 765
 766

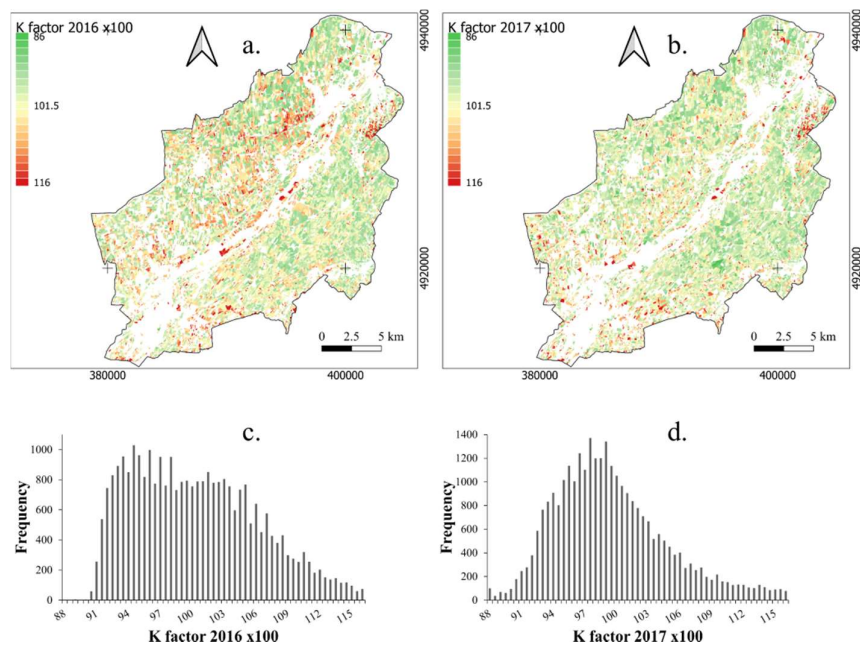
767 Figure 4. Map of NDVI anomaly in the area: a. Anomaly map for the year 2016; b. Anomaly
 768 map for the year 2017. Anomaly was computed at crop class level and then mosaicked to
 769 generate the map shown in figure. (Reference system is WGS 84 / UTM zone 32N, EPSG:
 770 32632).



771

772

773 Figure 5. Map of $k(x,y,t)$ factor (x 100) given for the 4 investigated crops (wheat, corn,
 774 ryegrass and meadows). a. $k(x,y,t)$ maps for the year 2016; b. $k(x,y,t)$ maps for the year 2017;
 775 c. frequency distribution of $k(x,y,t)$ in the year 2016 in the area of interest; d. frequency
 776 distribution of $k(x,y,t)$ in the year 2017 in the area of interest. $k(x,y,t)$ was computed at crop
 777 class level and then mosaicked. (Reference system is WGS 84 / UTM zone 32N, EPSG:
 778 32632).



779